Anti-cancer, Anti-invasiveness & Anti-metastasis of Green Engineered Bioorganic-Capped Silver Nanoparticles Fabricated from *Juniperus chinensis* Extract and Comparison to Cisplatin in Lung Cancer Cells (A549): In Vitro Assessment of Cellular and Molecular Pathways

Hassan Noorbazargan (h.noorbazargan@gmail.com)
Shahid Beheshti University of Medical Sciences School of Medicine https://orcid.org/0000-0003-1889-0139

Ainaz Mashayekhi
Islamic Azad University

Nazanin Khayam
Islamic Azad University

Mohammad Naghizadeh
Islamic Azad University

Amir Mirzaie
Islamic Azad University

Aghigh dolatabadi
Islamic Azad University

Pooria moulavi
Islamic Azad University

Sobhan amintehrani
Islamic Azad University

Mahsa kavousi
Islamic Azad University

Original article

Keywords: Juniperus chinensis, Human lung cancer cells, Green synthesized AgNPs, apoptosis, metastasis

Posted Date: October 9th, 2020

DOI: https://doi.org/10.21203/rs.3.rs-88253/v1

Version of Record: A version of this preprint was published at AMB Express on April 26th, 2021. See the published version at https://doi.org/10.1186/s13568-021-01216-6.

Abstract

The current study reveals anti-cancer properties of bio-functionalized silver nanoparticle (AgNPs) fabricated by *Juniperus chinensis* leaf extracts due to it's easy, low cost, biological activity, eco-friendly and lower side effects. The characteristics of AgNPs were determined by scanning electron microscopy [1], transmission electron microscopy (TEM), UV-visible spectroscopy, Fourier transform infrared (FTIR) spectroscopy, X-ray diffraction, Dynamic light scattering (DLS), Zeta potential and X-ray spectroscopy (EDX). Further, this study highlights the cellular and molecular mechanisms of AgNPs involves in anti-proliferative and apoptotic effect on human lung cancer cells (A549) and compared to commercial drug cisplatin by various biological methods such as MTT, flow cytometery analysis, gene expression patterns, migration and invasion inhibition, ROS and caspase production and cell staining. The size of AgNPs fabricated in this study was 12.96 with spherical shape and negative zeta potential. Up-regulation of capase 3,9 and p53, Annexin V-FITC/PI, DAPI staining, ROS production indicated remarkable apoptotic effect of AgNPs than cisplatin. Also down-regulation of MMP2/MMP9 scratch and matrigel assays revealed anti-metastatic properties of AgNPs.cell cycle analysis and down regulation of cyclin D1 showed cancer cell cessation in the G0/G1 phase. Overall results in current experiment revealed AgNPs synthetized by biogreen method anti-metastasis and anti-proliferation effect on lung cancer cells comparison to cicplatin drug and also had lower side effect on normal cell line.

Introduction

Silver nanoparticles are one of the preferable nanomaterials that progressively becoming a section of human daily lives.[2]. Recently AgNPs thanks to their marvelous and unparalleled nano-related features, have been applied extensively in different fields of science especially in biomedical field and have also been studied for their antimicrobial effects[1], wound healing[3] and anticancer [4] activity. A variety of procurement techniques are utilized for the synthesis of silver nanoparticles, among these methods, the usage of plant extracts are more attractive due to the availability of more biological entities, eco-friendly procedures, cost-effective, abundantly renewable, and safe nature for human therapeutic use [5]. A huge data evidenced numerous phytochemicals compounds such as flavones, lignins, and terpenes present in different parts of plants have been identified that are triggered in anti-microbial and anticancer activities of phyto-synthesized AgNPs[6].

AgNPs are being utilized for treating different types of cancerous cells due to their especial and particular extraordinary biomedical applications (anti-cancer, anti-bacterial, anti-viral and anti-angiogenic properties) and their surface specific features[7]. Various studies indicated the apoptotic effect of silver nanoparticles on colon cancer HT29 cell line29[8], as well as the cytotoxic effects and anticancer activity of phyto-synthesized silver nanoparticles on breast cancer MCF-7 cell line [9]and HeLa cervical cancer cells[10]. Further studies on mouse model with tumor revealed that the AgNPs can significantly expand the survival time in comparison with tumor controls and consequently show satisfactory antitumor and anti-angeogenic effect[11]. The biological results acquired from researches showed anti-cancerous and anti-proliferative activity of biologically synthesized silver nanoparticle lung cancer A549 cells and non-

cytotoxicity were observed due to its ability to arrest the cell cycle at G1 phase[12]. The evidence obtained from one study confirms that bio-sythesized AgNPs using the *Juniperus chinensis* leaf showed the potent anticancer effect on the human adenocarcinoma gastric (AGS) cell lines[13].

Cisplatin is a chemotherapy medication used to treat a number of cancers such as bladder cancer, head and neck cancer, esophageal cancer, lung cancer, mesothelioma, brain tumors and neuroblastoma. Its serious side effects include numbness, trouble walking, allergic reactions, electrolyte problems, and heart diseas. This drug works in part by binding to DNA and inhibiting its replication[14, 15]. Hence, this study was conducted to analyze the anticancer effects of green-synthesize AgNPs using *Juniperus polycarpos* on A549 (adenocarcinomic human alveolar basal epithelial cells) cell lines, as well as comparison of this synthetic AgNPs with Cisplatin commercial drug.

Methods

1. Plant materials and compounds extraction

The plant leaf of *Juniperus polycarpos* were obtained from the Plant Bank - Iranian Biological Resource Center. Leaves were dried under direct sunlight for 48 hours and ground to make a fine powder using a stainless blender. The powder was exposed to 500 mL of 80% methanol (MeOH) for 12 hours. Then the extract was subsequently filtered and concentrated using a vacuum rotary evaporator at 40 °C giving semi-solid extracts and were maintained at 4 °C for applying on cancer cells.

2. AgNPs phyto-synthesis and characterization

0.01 molar silver nitrate was weighted, then 40 ml of distilled water and 4 ml of plant extracts were added and shaken vigorously. After one day, Change in colour of the solution to dark brown colour were monitored to determine nanoparticles formation. The preparations were then centrifuged at 13000 rpm for 10 min. Supernatants were discarded and the pellet was washed twice in 10 ml of distilled water to remove any contaminating plant material and centrifuged at 13000 rpm for 15 min again. At least, the mixture was dried at 37 °C for 24 h to come in powder form.

X-ray diffraction (XRD) (PW3710, the Netherlands) with CuKα radiation (λ = 0.0260 nm) and Fourier-transform infrared spectroscopy (FTIR technique) were applied for the crystal phase analysis of the AgNPs powders. The synthesis of AgNPs was measured using a UV-1800UV–spectrophotometer (Shimadzu, Japan). The particles size, morphology and distribution were detected using scanning electron microscopy [1] (LEO SEM 1450VP, UK) and transmission electron microscopy [8] (FEI 5022/22 Tecnai G2 20 STwin, CR) and Energy Dispersive Spectroscopy (EDS).

3. A549 Cells culture

The human lung cancer A549 cell line was purchased from Iranian Biological Resource Center. The cell lines A549 (ATCC) were cultured at 37 °C and in a 5% CO2 in air atmosphere. All cells tested negative for mycoplasma contamiinations and were markedly cultured in fresh medium (RPMI1640) supplemented

with 10% fetal bovine serum (FBS, DENAzist Asia's Co) and 1% antibiotics (penicillin/streptomycin). The cells (1 × 106 cells/ml) were plated in T-25 flasks containing 5 mls of RPMI1640 and grown in a humidified incubator under an atmosphere of 95% air and 5% CO2 at 37 °C to subconfluence (90–95%). The culture medium was replaced every 48 hours. Once the cells reached 90–95% confluency, the medium was aspirated, and the cells monolayer was washed three times with sterile phosphate buffered saline. The cell monolayer was treated with 1 ml of 0.25% (w/v) trypsin-EDTA and incubated briefly at 37 °C and visualized microscopically to ensure complete cell detachment. Cells were re-suspended in complete growth medium. Cells were also stained with trypan blue (100 µl of cell suspension and 100 µl of 0.4% trypan blue), incubated for 2 minutes at room temperature, and counted using a hemacytometer. The cells were seeded at a density of 1 × 104 cells/ well in 96-well microtiter tissue culture plates prior to Vascum album different extracts treatment (33)

4. Cytotoxicity assay of AgNPs

The MTT [3-(4,5-dimethylthiazol-2-yl)-2,5-diphenyltetrazolium bromide] assay was performed for assessing cell proliferation activity and cytotoxicity in A549 cells exposed to different concentrations of bio-synthesized AgNPs and cisplatin. Cell viability was determined using the MTT assay 24 hours after incubation. The basis of MTT assay is based on reduction of a tetrazolium component (MTT) into an insoluble formazan product by succinate dehydrogenase activities in mitochondria. The Protocol of MTT assays were conducted according to standard protocols in 96-well plates. A549 cells were seeded in 96-well plates with 1×10^4cells/well and placed at 37 °C in a 5% CO2 humidified incubator until 60% confluency.

The complete growth medium was removed and the cells were exposed to serum starvation for 24 h prior to treatment. Cells cultures were incubated in culture medium for 2 h alone served as control (untreated cells) for evaluating cell viability. The cells were treated with different doses of 0.78, 1.56, 3.125, 6.25, 12.5, 25, 50 and 100 µg/ml of bio-synthesized AgNPs and 3.125, 6.25, 12.5, 25, 50 and 100 µg/ml of cisplatin, the medium was removed and MTT solution (100 µl) were added to each well and incubated for 4 h. The plates were incubated under 95% atmosphere air and 5% CO2 at 37 °C for 4 h. The MTT solution was removed and 200 µl aliquots of DMSO were added to each well to dissolve the formazan crystals followed by incubation for 10 min at 37 °C. Treatments were performed in triplicates, and optical densities were read at 570 nm by spectrophotometric method (34). IC50 of AgNPs and cisplatin on A549 cell lines were calculated by the statistical package, Pharm-PCS software.

5. Evaluation of caspase-3, caspase-9, MMP2 and MMP9 genes expression by Real-time PCR

RNA extraction from cells was performed using RNX kit (SinaColon Co) according to the manufacturer's instructions. The absorbance of a RNA sample was measured at 260 and 280 nm by a spectrophotometer for calculating RNA concentration and purity. RNA quality was assessed by gel electrophoresis method on a 1.2% agarose gel for 1 h at 100 V. Genomic DNA was removed by RNase-free DNase I (Thermo Scientific). The cDNA synthesis reaction was carried out with Fermentas First Strand

cDNA Synthesis Kit by RT-PCR method on two µg of the treated RNA, according to the manufacturer's instructions. Agterwards, 1 µg of cDNA was applied for assessment of genes expression using specific primers (Table1).

The amplification was carried out in a reaction volume of 25 µL including 12.5 µl SYBR Green kit (Amplicon, Denmark), 1 µl cDNA, and 1 µl of each primer (Table 1) on Exicycler™ 96 - Bioneer (South Korea). β-actin gene has been used as an internal control. In current study, the $2^{-\Delta\Delta CT}$ method was applied to survey the relative changes in genes expression from real-time quantitative PCR experiments. Data analysis was performed with SPSS statistical analysis software and the results were analyzed by One-way Analysis of Variance (ANOVA) and Tukey's post hoc-test to determine significant difference between treatments ($P < 0.05$).

Table 1
Primer sequence designated for RT-PCR.

gene	Primer sequence
Casp3	Forward: 5'- CATACTCCACAGCACCTGGTTA-3'
	Revers: 5'- ACTCAAATTCTGTTGCCACCTT-3'
Casp9	Forward: 5'-CATATGATCGAGGACATCCAG-3
	Revers: 5'-TTAGTTCGCAGAAACGAAGC-3'
MMP2	Forward: 5'- F: TTG ACG GTA AGG ACGGAC TC-3'
	Revers: 5'-CATACTTCACACGGACCACTTG – 3'
MMP9	Forward: 5'- GCACGACGTCTTCCAGTACC – 3'
	Revers: 5'- CAGGATGTCATAGGTCACGTAGC – 3'
b-actin	Forward: 5'- TCCTCCTGAGCGCAAGTAC-3'
	Revers: 5'- CCTGCTTGCTGATCCACATCT-3'
Cyclin D1	Forward: 5'- CAGATCATCCGCAAACACGC-3'
	Revers: 5'- AAGTTGTTGGGGCTCCTCAG-3'
P53	Forward: 5'- TAACAGTTCCTGCATGGGCGGC -3'
	Revers: 5'- AGGACAGGCACAAACACGCACC -3'

6. Apoptosis assay of AgNPs

The apoptotic toxicity level to the A549 cells was determined by Annexin- V-FITC/propidium iodide staining. According to the manufacturer's instructions, the cells were treated with AgNPs and cisplatin for 24 h. Afterwards, the cells were harvested and centrifuged at 200 × g and suspended in appropriate

buffer. Following that, 5 µL Annexin-V-FITC labeling and 5 µL PI solutions were added to the mixture, which were then incubated for five minutes at 25 °C and analyzed with flow cytometry (Bd, UK).

7. Cell cycle analysis

Cell cycle analysis 5×10^5 A549 cells (cells/mL) were treated with *Juniperus polycarpos* leaf extract NPs and cisplatin for 30 min. The cells were washed and fixed with 500 µL of ice-cold 70% ethanol and refrigerated for 1 h prior to staining. The cell pellet was washed and re-suspended in 200 µL of Guava Cell Cycle reagent containing PI and incubated in the dark at room tem perature for 30 min before analysis with Guava® easyCyte. For each step, centrifugation was performed at 5000 rpm for 5 min at room temperature. The data obtained were analyzed using Incyte software.

8. Scratch wound healing assay

Cells were seeded in a 6-well culture plate and allowed to reach 70–80% confluence as a monolayer before they were transfected with siRNAs. The scratch was vertically introduced to the cells in the monolayer using a 10 mL pipette tip. All the images were captured using OPTIKA B-353-PLi (Italy) microscope system at the respective time points. Each condition was assessed in triplicate and was independently repeated three times.

9. Matrigel invasion assay

The cell invasion assay was performed using a 24-well Transwell chamber with a pore size of 8 lm (Corning, ME). The inserts were coated with 100 ll Corning Matrigel basement membrane matrix (final concentration of 200 mg/mL, Corning, MA). Twenty-four hours after the transfection, cells 10^5 were trypsinized, and cells in 100 ll of serum-free medium were transferred to the upper matrigel chamber and incubated for 18 h. A medium supplemented with 20% FBS was added to the lower chamber as the chemoattractant. After incubation, the cells that passed through the filter were fixed with Methanol and stained with Giemsa. The number of invaded cells was counted in 5 randomly selected high-power fields under the microscope.

10. Reactive oxygen species (H2-DCFH-DA) assay

A549 human lung epithelial adenocarcinoma cells were cultured in minimum essential medium (Hyclone Laboratories, Logan, UT, USA) containing 10 µM H2- DCFDA in a humidified incubator at 37 °C for 30 min. Cells were washed twice with warm PBS (pH 7.4) and were lysed on lysis buffer (25 mM HEPES [pH 7.4], 100 mM NaCl, 1 mM EDTA, 5 mM MgCl2, and 0.1 mM DTT containing EDTA-free protease inhibitor cocktail (Roche)). Cells were cultured on coverslips in a 4-well plate. Cells were incubated in DMEM containing 10 µM H2-DCFDA at 37 °C for 30 min. Cells were again washed in PBS and were mounted with VECTASHIELD Mounting Medium for fluorescence with DAPI (Burlingame, CA, USA), and were imaged with a fluorescence microscope.

11. Caspases activity

The activity of proteases caspases was detected using the caspase-3 (ab39401) and caspase-9 (ab65608) kits purchased from Abcam (Cambridge, UK). caspases 3 and 9 recognize the sequence DEVD and LEHD, respectively, and cleave from the labeled substrate p-NA emitting light, which was quantified using a spectrophotometer at 405 nm.

Results

Characterization of Synthetized Silver Nanoparticles using *Juniperus polycarpos*

Change in color of solution with Juniperus polycarpos extract was apperceived after incubation of flask containing $AgNO_3$ at 37º C for 24 hours. The color of the extract solution altered from light yellow to dark brown after 24 hours. The alteration in color indicates the accepted synthesis of silver nanoparticles. AgNPs formation also was verified using UV-vis, XRD, FTIR, EDS, SEM and TEM.

UV-vis analysis

Figure 1 shows the recorded UV-Vis absorption spectra of the synthesized AgNPs by *Juniperus polycarpos* extract. For UV–vis analysis, the absorption of NPs was detected in 438 nm wavelength in UV–vis spectrum. Moreover, no additional peaks were noticed in the spectrum, which revealed great purification of synthesized AgNPs .

Characterization of size, morphology and DLS analysis of AgNPs

SEM and TEM images of AgNPs formed by *Juniperus polycarpos* indicate the shape, size and morphology of nanoparticles. According to microscopically investigation the green synthesized AgNPs at optimal conditions had maximum average size of 10–50 nm with mean size of 12.96 nm (Fig. 2).

According to the DLS analysis, the average size of AgNPs was estimated 133.4 nm and Polydispersity Index (PdI) value was recorded at 0.254.

The silver nanoparticles were found to be well, monodispersed from each other and spherical-shaped based on TEM and low pdl value of DLS analysis (Fig. 2c).

XRD, EDX & Zeta potential

The XRD patterns of the AgNPs synthesized by *Juniperus chinensis* extract, four intense XRD peaks were indicated at 2θ = 38.6, 44.4, 64.6, and 77.1correspond to the (111), (200), (220), and (311) crystallographic planes of facecentered cubic (FCC) structure.

Figure 3b shows the EDS analysis of *Juniperus polycarpos* mediated synthesis of silver nanoparticles. The EDS technique detects a potent signal at 3 keV indicates the presence of elemental silver. EDS

analysis indicates the elemental analysis of the nanoparticles in which the percentage of silver ions was 99.15%.

In the current study, the fabricated AgNPs had a negative zeta potential of − 9.76 mV, indicating higher stability of the bio-functionalized AgNPs (Fig. 3c). The greater negative surface charge potential value indicates that the synthesized AgNPs are high dispersed in the medium with long-term stability [16].

The negative potential value may be due to the reducing and capping substances especially fatty acid in *Juniperus chinensis* extract also the aggregation of the nanoparticles could be prevented by electrostatic repulsion between negative charge of the nanoparticles [17, 18].

Fourier Transform Infrared Spectroscopy (FT-IR) analysis

The result of FTIR analysis of bio-synthesized AgNp revealed different stretches of bonds at different peaks. The strong and broad peak at 3411.89 cm-1 was related to the stretching vibrations of the O-H and N-H groups in the extracted. Absorption peaks located at 1619.28 cm − 1 and 1385.60 cm − 1 are assigned to C = C and C–H bend alkane groups, respectively. Peak at 1112.81 cm − 1 associated with C–O–C stretch ethers, while 621.51 cm − 1 represents = C-H group in alkenes and aromatic compounds. Peak at 2925.16 cm − 1 corresponds to aliphatic C–H group.

Cell Viability and MTT Test Results

The possible cytotoxicity results of various cisplatin concentrations and AgNPs on HEK293 cells (obtained from National Cell Bank (NCBI) of Pasteur Institute of Iran), as a normal cell line, and A549, as a cancerous cell line, indicated that plant extract and AgNPs have cytotoxic effects against cancerous cell line while not toxic to the normal cells in lower concentrations(Fig. 5). It was also detected that the maximum cell death was belong to synthesized AgNPs, which was 35% for the cultured HEK293 cells after 24-hour exposure. This is when cisplatin resulted in 60% cytotoxicity toward the HEK293 cells. However, the cytotoxicity of AgNPs and the cisplatin against MCF-7 tumor cell line were approximately 60% and 40%, respectively (at the concentration of 12.5 µg/mL). As can be seen in Fig. 5, the toxicity of AgNPs is dose-dependent.

Figure 5A and 7C indicate viability of A549 and HEK293 cells exposed to 0.78, 1.56, 3.125, 6.25, 12.5, 25, 50 and 100 µg/ml of bio-synthesized AgNPs in cell culture. There was no significant difference between viability of HEK293 cells exposed to 0.78, 1.56, 3.125, 6.25, 12.5 and 25 µg/ml of AgNPs. However, HEK293 cells viability remarkably decreased in groups exposed to 50 and 100 µg/ml of AgNPs compared to control cells ($P < 0.05$ and $P < 0.01$, respectively). The reduction in A549 cells viability was observed when exposed to 3.125 and 6.25 µg/ml of AgNPs($P < 0.05$ and $P < 0.01$, respectively). There was also statistically significant difference between viability of A549 cells exposed to 12.5, 25, 50 and 100 µg/ml of biosynthesized AgNPs($P < 0.001$). For A549 and HEK293 cell lines the IC50 values by cultivation in the presence of silver nanoparticles were calculated 9.87 and 111.26 µg/ml, respectively.

Figure 5B and 5D also shows viability of A549 and HEK293 cells exposed to 3.125, 6.25, 12.5, 25, 50 and 100 µg/ml of cisplatin in cell culture. A549 cells viability significantly declined in groups exposed to 50 and 100 µg/ml of cisplatin compared to control cells ($P < 0.001$). Exposure of A549 cells to 6.25 ($P < 0.05$), 12.5 and 25 ($P < 0.01$) µg/ml of cisplatin also led to significant decrease in viability of A549 cells. However, there was no significant difference between viability of A549 cells exposed to 3.125 µg/ml of cisplatin compared to control cells. HEK293 Cell viability decreased greatly after exposure to 12.5 ($P < 0.05$), 25, 50 ($P < 0.01$) and 100 ($P < 0.001$) µg/ml of cisplatin. However, no significant differences were observed in the HEK293 cells viability at low doses (3.125 and 6.25 µg/ml) of cisplatin. The IC50 values of cisplatin determined for A549 and HEK293 cell lines were 24.67 and 43.35 µg/ml, respectively.

Gene expression

Figure 6 show the induction expression levels of caspase-3 and caspase-9 genes treated by AgNPs. According to Fig. 8a, the expression levels of caspase-3 and caspase-9 in cells exposed to synthetic AgNPs were higher than cisplatin treated cells. The results also revealed that AgNPs can down-regulation the expression levels of MMP2 and MMP9 in A549 cells which higher than cisplatin effect. Our result also was shown in Fig. 8c indicates the up-regulation of p53 and reduction of cyclin D1 in both AgNp and cisplatin treated A549 cells.

Flow cytometric Apoptosis analysis

To subsequent characterize apoptosis induction of AgNPs, A549 cells were stained with Annexin-V/PI assay, followed by flow cytometry test. The determination finding of flow cytometry assay was demonstrated in Fig. 10. The flow cytometry data obviously indicated that biosynthesized AgNPs can stimulate cell death procedure in A549 cells. Based on the Annexin V-FITC/PI staining, 96.1% of control cells were detected viable with early apoptotic value of 0.84%, late apoptotic value of 1.1%, and necrotic value of 1.9% of cells, which are common process for cells can be proliferated in culture mediums. The A549 cells exposed to AgNPs dramatically induced the late apoptotic and necrotic cells as compared with untreated control cells. An increase in the percentage of apoptotic (early and late, Q2 + Q3) cells was detected with the value of 34.4 and 16.08% for ic50 of synthetic AgNPs and cisplatin, respectively. AgNPs significantly ($p < 0.001$) has lower necrotic effects (Annexin V -/PI+) (4.0%, Q1) in A549 cells at ic50 concentrations than cisplatin (Annexin V -/PI+) (13.4%, Q4), indicative of apoptotic cell death and side effects of cisplatin drug (Fig. 7).

Cell cycle analysis

To indicate the distribution of *Juniperus polycarpos* leaf extract AgNps and cisplatin-treated A549 cells in different phases of the cell cycle, the DNA content in cells was detected by PI staining and analyzed by flowcytometry. The results indicated that the treatment with both AgNPs and cisplatin led to an increase in the population of cells in the G0/G1 phase (Fig. 8). The results showed that 15.58% and 7.58% of the cells treated with nanoparticles and cisplatin respectively were recorded in the sub-G1 phase.

Inhibition of migration and invasion of A549 cells

Scratch wound healing assay

To examine the anti-metastatic properties of each drug, a scratch wound assay was performed in all three cell lines. A wound healing assay was performed to exclude the growth inhibitory effect of AgNPs and cisplatin on migration. The effect of AgNPs and cisplatin on A549 cells was detected, and it was identified that both AgNPs and cisplatin have great effects on cells migration. The results of the wound healing assays are presented in Fig. 9. The area that the cells had migrated (toward the initially scratched midline, from the border line) was measured. The cells incubated with AgNPs migrated across an area that was less than that of the cells incubated with the cisplatin and control medium, indicating that both AgNPs and cisplatin weaked the migration of the A549 cells.

Figure 9A Indicates the migration rate in control cells, B, shows the migration rate in A549 cells were treated with AgNPs and C, revealed the migration rate A549 cells were treated with cisplatin for 24 h. Migration ability was determined by the migration rate of migrating cells at 24 h.

Invasion assay

We accessed the effects of both AgNPs and cisplatin on invasion ability of A549 cells. As shown in Figs. 13, both AgNPs and cisplatin inhibited the migration dramatically compared with the control group. AgNPs and cisplatin decreased the migration ability from 85–30% and from 85–50%, respectively (Fig. 10).

Induction activation of caspases and ROS

Caspases are the cysteine-aspartate proteases that play an important role in apoptosis. Caspase-3 is the initiator caspase and caspase-9 is the executor caspase. The executor caspase expression level was increased in A549 lung cancer cell lines treated with both AgNPs and cisplatin but the caspase-3 expression level had significant increased only in cells treated with AgNPs (Fig. 11A). The intracellular ROS content of control, cisplatin and AgNPs treated A549 cells is depicted in Fig. 11B. Forty percent and 90% increase in ROS content were observed in cisplatin and AgNPs-treated cells, respectively.

Determination of Apoptotic Effects in A-549 Cells

Apoptotic pathway or programmed cell death includes several changes in cells which contains morphology of cells, chromatin condensation, DNA, and nuclear fragmentation [35, 37]. In order to comparison the effect of AgNPs and cisplatin on cell death in A549 cells, nuclei of the cells were stain by DAPI stain. As shown in Fig. 12, higher levels of nuclear fragmentation, disintegration and condensation of chromatin at the boundary of the nuclear membrane and cell death were seen in AgNPs treated cells, compared to cells treated with cisplatin[19].

Discussion

Cancer is a leading cause of death worldwide, accounting for an estimated 9.6 million deaths in 2018[20]. Lung cancer is the most universally occurring cancer in men and the third most commonly occurring

cancer in women, contributing about 11.6% of the total cancer incidence burden[20]. Natural compounds propose benefits over synthetic drugs, including low side effects, so medicinal herbs have long captured the attention of researchers[21]. In the current investigation, the anticancer effects of green-synthesize AgNPs using *Juniperus polycarpos* on A549 (adenocarcinomic human alveolar basal epithelial cells) cell lines was assayed. Additionally, the expression of apoptotic and metastatic genes including caspase-3, caspase-9, MMP2 and MMP9 was evaluated.

According to results, AgNPs have been efficiently synthesized using *Juniperus polycarpos* extract, which SEM, TEM, XRD, UV-vis, EDS and FTIR methodes confirmed the changes in the chemical composition, morphology and size of the Ag nanoparticles. *Juniperus polycarpos* is economically cheap and easily available and AgNPs are obtained from nature can act as both reducing and capping agent. Recently, recent studies indicated that herbal extracts have been applied for the green synthesis of AgNPs[22]. The specific mechanism of silver nanoparticles bioreduction is not fully understood yet but various investigations suggested the mechanism of metallic nanoparticle synthesis using plant extracts. There exist several biomolecules in plants which are engaged in reduction and biosynthesis of metal nanoparticles[23].

MTT assay was carried out to survey the in vitro cytotoxic trait of biosynthetic AgNPs and cisplatin drug. A549 cells were treated with different concentration of synthesised AgNPs and cisplatin for 24 h to establish the inhibitory percentage against cancer treated and untreated cell lines. Our study findings showed that the cancer and normal cells viability were clearly proportionate to the concentration of the AgNPs. When the IC50 of the AgNPs and cisplatin was compared, the synthesised AgNPs showed lower percentage of inhibition of cells proliferation at lower concentration against the A549 cancer cells than the cisplatin. At lower concentrations the AgNPs demonstrate remarkable toxicity on the growth of A549 cells but the cell viability did not reduce significantly with lower concentrations of drug. The results of the MTT assays also showed that AgNPs exhibited the lower cytotoxicity against HEK293 cells than cisplatin, which indicated that exposure to the cisplatin was associated with increased cell death and cisplatin-DNA intra-strand crosslinks result in cytotoxicity due to the presence of the platinum in its structure[24]. The analysis demonstrated that the anticancer activity of synthesized AgNPs mainly show a dose–response relationship and cytotoxicity increased at higher concentrations. Among the nanoparticles, AgNPs were found to be best for inhibition of cancer cell proliferation[25]. It might be due to the synergetic properties of bio-molecular groups derived from *Juniperus polycarpos* that held in nanoparticles formation procedure. This is the first comparative investigation to introduce the cytotoxicity of phyto-synthesised AgNPs using *Juniperus polycarpos* extract and cisplatin drug against A549 cells. We believed that phyto-synthesis of AgNPs could lead ultimately to apoptotic cell death, DNA damage and the cell morphology alterations[26].

Considering the importance role of these genes in apoptotic and necrotic pathway, the Real-time PCR results indicate that caspase3- and caspase-9 genes expression levels were induced with both exposure to Ic50 of synthetic AgNPs and cisplatin. AgNPs also is more powerful to decrease expression of MMP2 and MMP9 genes than commercial drug. Various in vitro reports indicates that biogenic AgNPs decreased

the mRNA and protein expression of MMP-2 and MMP-9 in wounded granulation tissues[27]. A huge amount of studies show treating MCF-7 cancer cells with AgNPs induces apoptosis by inducing the release of cytochrome c, production of reactive oxygen species [1], and activation of the caspase-3 pathway[28].

Further investigation included the annexin V/PI assay, followed by flow cytometry. In the early apoptosis stage, alterations take place at the cell surface and phosphatidylserins (PS) in the membrane is translocated from the inner to the outer leaflet of the plasma of cell membrane. Annexin–V with PI staining could be used for detection of PS exposing cells via flow-cytometry method. The groups of cells resident in the Annexin V+/PI- and the Annexin V+/PI + were identified as the early and late stage of apoptosis, respectively. [29]. The staining results showed The A549 cells exposed to AgNPs significantly increased the early and late apoptotic and necrotic cells as compared with untreated control cells. In contrast, the early, late apoptotic cell percentages cells treated with AgNPs were found to be higher than cisplatin treatments, while the percentages of necrotic cell (Annexin V−/PI+) was lower than the treatment with cisplatin. This results indicated that AgNPs is more effective in apoptosis and has lower necrotic effects on cells than cisplatin drug.

The anticancer action of silver nanoparticles is due to wide spectrum of biological activities in cancer cells cycle proliferation, which resulted in deprived of cancer cells ability for division and growth[30]. Our data suggest that the treatment of A549 cells with biosynthesized AgNPs resulted in considerable sub-G1 phase deterrence of cell cycle proliferation, showing one of the mechanisms by which the AgNPs may act to suppress cancer cell viability and tumor growth. The reduction in cells population treated with the AgNPs and cisplatin was observed in G2 and S phase, whereas the cell population in the sub- G1 phase was enhanced when compared with controls. These data imply that both biosynthesized AgNPs and cisplatin progressed cell cycle development in the sub G1 phase arrest.

Since tumor cell migration and invasion is required for cancer metastasis, wound healing, scratch, and invasion assays were conducted to assess the progression of cancer cell development in A549 cell lines, following treatment with AgNPs and cisplatin, which the results were shown all cell lines treated with AgNPs and cisplatin invaded and migrated, but the antimigratory effect of AgNPs in A549 cells was significantly higher than cisplatin treated cells and control. These results proved that our targeted drug-loaded nanoparticle can be used effectively in lung cancer cell lines.

Various NP particularly AgNPs can stimulate oxidative stress through ROS generation, which may induce apoptotic pathway in reaction to different signals and pathophysiological conditions[31, 32]. Several studies have indicated the roles of numerous metal NPs including AgNPs in induction of ROS generation in many cell lines [32, 33]. AgNPs have been considered as one of the most potent candidates in medical application of nanotechnology via ROS production[34]. In this assay, we have reported that significant increase in ROS content were observed in cisplatin and AgNPs-treated cells, respectively, which indicates the initiation of apoptosis by the biosynthesized AgNP.

The current study indicate Up-regulation of p53 in A549 cells under treatment of AgNp that can arrest cells in a sub-G1 phase cell cycle and prepare cells for induction apoptosis. Down-regulation of cyclin D1 stop cells at the G0/G1 phase and prevents cell progression to next phases and by increasing capase 3/9 evokes apoptosis in arrested cells [35–37].

Conclusion

This is the earliest investigation to develop economical, simple, and eco-friendly procedure for bio-synthesis of silver nanoparticles using *Juniperus polycarpos* extract as reducing agent. AgNPs were synthesized and characterized using UV–vis spectroscopic, XRD analysis, SEM, EDS, TEM and FT-IR; these process evidenced the presence of AgNPs with an average size of 38.8 nm. The bioprepared AgNPs demonstrated greater favorable anticancer potential than cisplatin drug and can be utilized in pharmaceutical industries. The AgNPs were demonstrated as considerable apoptosis inducing and metastatic reducing agents against cancer cell lines. The phyto-synthesised AgNPs have potent cytotoxic activity against A549 cell line compared with cisplatin drug. Moreover, the Annexin V/PI staining, cell cycle analysis, wound healing assay, cell migration and invasion assay, production of caspases and ROS strains results indicated the AgNPs-induced cytotoxicity reduced A549 cells viability, which is referred to capability of AgNPs to stimulate apoptosis pathway rather than necrosis. Therefore, subsequent investigations are required to quietly clarify the mechanism of action of silver nanoparticles toxicity against cancer cell lines.

Declarations

Acknowledgements

The authors would like to acknowledge the laboratory of Islamic Azad University.

Disclosure statement

The authors declare that they have no conflict of interest.

References

1. A. M. Iniyan, R. R. Kannan, F.-J. R. S. Joseph, T. R. J. Mary, M. Rajasekar, P. C. Sumy, A. M. Rabel, D. Ramachandran and S. G. P. Vincent (2017) Microbial pathogenesis 112:76-82
2. M. Singh and T. Sahareen (2017) LWT 86:116-122
3. L. C. Yun'an Qing, R. Li, G. Liu, Y. Zhang, X. Tang, J. Wang, H. Liu and Y. Qin (2018) International journal of nanomedicine 13:3311
4. M. P. Patil and G.-D. Kim (2017) Applied microbiology and biotechnology 101:79-92

5. V. Kumar and S. K. Yadav (2009) Journal of Chemical Technology & Biotechnology: International Research in Process, Environmental & Clean Technology 84:151-157
6. K. Gopinath, S. Kumaraguru, K. Bhakyaraj, S. Mohan, K. S. Venkatesh, M. Esakkirajan, P. Kaleeswarran, N. S. Alharbi, S. Kadaikunnan and M. Govindarajan (2016) Microbial pathogenesis 101:1-11
7. A.-C. Burdușel, O. Gherasim, A. M. Grumezescu, L. Mogoantă, A. Ficai and E. Andronescu (2018) Nanomaterials 8:681
8. F. Ghanbar, A. Mirzaie, F. Ashrafi, H. Noorbazargan, M. D. Jalali, S. Salehi and S. A. S. Shandiz (2016) IET nanobiotechnology 11:485-492
9. K. Venugopal, H. Rather, K. Rajagopal, M. Shanthi, K. Sheriff, M. Illiyas, R. Rather, E. Manikandan, S. Uvarajan and M. Bhaskar (2017) Journal of Photochemistry and Photobiology B: Biology 167:282-289
10. E. S. Al-Sheddi, N. N. Farshori, M. M. Al-Oqail, S. M. Al-Massarani, Q. Saquib, R. Wahab, J. Musarrat, A. A. Al-Khedhairy and M. A. Siddiqui (2018) Bioinorganic Chemistry and Applications 2018
11. Y. He, Z. Du, S. Ma, Y. Liu, D. Li, H. Huang, S. Jiang, S. Cheng, W. Wu and K. Zhang (2016) International journal of nanomedicine 11:1879
12. M. Annu, S. Ahmed, G. Kaur, P. Sharma, S. Singh and S. Ikram (2018) Toxicology research 7:923-930
13. K. Al-Dhafri and C. L. Ching (2019) Biocatalysis and agricultural biotechnology 18:101075
14. L. Galluzzi, L. Senovilla, I. Vitale, J. Michels, I. Martins, O. Kepp, M. Castedo and G. Kroemer (2012) Oncogene 31:1869-1883
15. H. Zhu, H. Luo, W. Zhang, Z. Shen, X. Hu and X. Zhu (2016) Drug design, development and therapy 10:1885
16. S. Mukherjee, D. Chowdhury, R. Kotcherlakota and S. Patra (2014) Theranostics 4:316
17. R. Vivek, R. Thangam, K. Muthuchelian, P. Gunasekaran, K. Kaveri and S. Kannan (2012) Process Biochemistry 47:2405-2410
18. S. Honary and F. Zahir (2013) Tropical Journal of Pharmaceutical Research 12:255-264
19. S. S. Azandeh, M. Abbaspour, A. Khodadadi, L. Khorsandi, M. Orazizadeh and A. Heidari-Moghadam (2017) Iranian journal of pharmaceutical research: IJPR 16:868
20. F. Bray, J. Ferlay, I. Soerjomataram, R. L. Siegel, L. A. Torre and A. Jemal (2018) CA: a cancer journal for clinicians 68:394-424
21. N. E. Thomford, D. A. Senthebane, A. Rowe, D. Munro, P. Seele, A. Maroyi and K. Dzobo (2018) International journal of molecular sciences 19:1578
22. S. K. Srikar, D. D. Giri, D. B. Pal, P. K. Mishra and S. N. Upadhyay (2016) Green and Sustainable Chemistry 6:34
23. S. Iravani, H. Korbekandi, S. V. Mirmohammadi and H. Mekanik (2014) Reviews in Advanced Sciences and Engineering 3:261-274
24. S. Manohar and N. Leung (2018) Journal of nephrology 31:15-25

25. S. Ghozali, L. Vuanghao and N. Ahmad (2015) C roseus,
26. H. Khalili, S. A. S. Shandiz and F. Baghbani-Arani (2017) Journal of Cluster Science 28:1617-1636
27. N. Krishnan, B. Velramar, B. Ramatchandirin, G. C. Abraham, N. Duraisamy, R. Pandiyan and R. K. Velu (2018) Materials Science and Engineering: C 91:146-152
28. A. G. Al-Nuairi, K. A. Mosa, M. G. Mohammad, A. El-Keblawy, S. Soliman and H. Alawadhi (2019) Biological trace element research:1-10
29. Y. Pan, W. Shan, H. Fang, M. Guo, Z. Nie, Y. Huang and S. Yao (2014) Biosensors and Bioelectronics 52:62-68
30. G. Raja, Y.-K. Jang, J.-S. Suh, H.-S. Kim, S. H. Ahn and T.-J. Kim (2020) Cancers 12:664
31. A. Abdal Dayem, M. K. Hossain, S. B. Lee, K. Kim, S. K. Saha, G.-M. Yang, H. Y. Choi and S.-G. Cho (2017) International journal of molecular sciences 18:120
32. M. Nita and A. Grzybowski (2016) Oxidative Medicine and Cellular Longevity 2016
33. A. Avalos, A. I. Haza, D. Mateo and P. Morales (2014) Journal of applied toxicology 34:413-423
34. A. El-Hussein and M. R. Hamblin (2016) IET nanobiotechnology 11:173-178
35. M. Rahimivand, F. Tafvizi and H. NoorBazargan (2020) International Journal of Biological Macromolecules,
36. N. N. Fard, H. Noorbazargan, A. Mirzaie, M. Hedayati Ch, Z. Moghimiyan and A. Rahimi (2018) Artificial cells, nanomedicine, and biotechnology 46:S1047-S1058
37. S. Aslany, F. Tafvizi and V. Naseh (2020) Materials Today Communications 24:101011

Figures

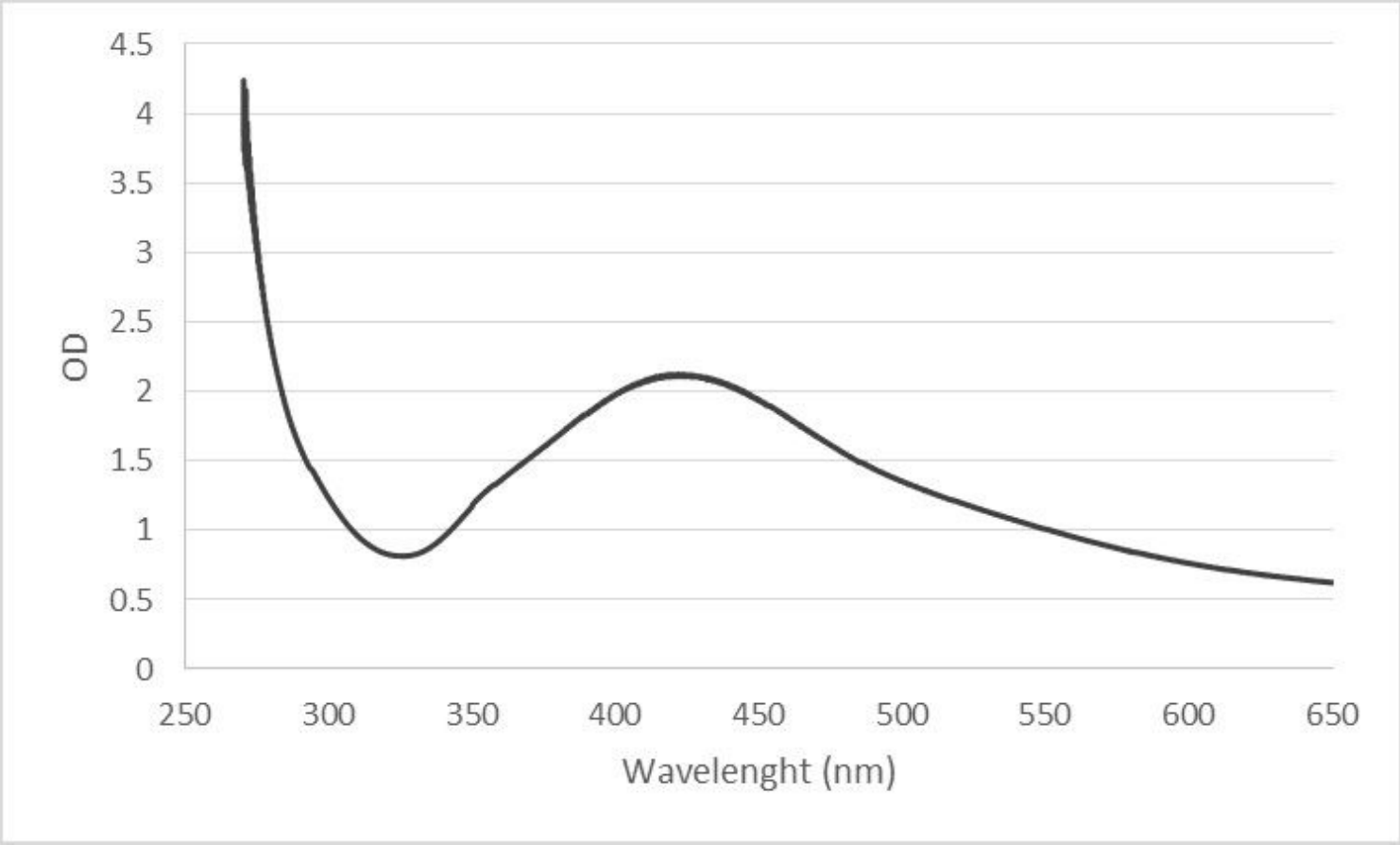

Figure 1

UV–visible spectrum of biologically synthesized silver nanoparticles during the reaction.

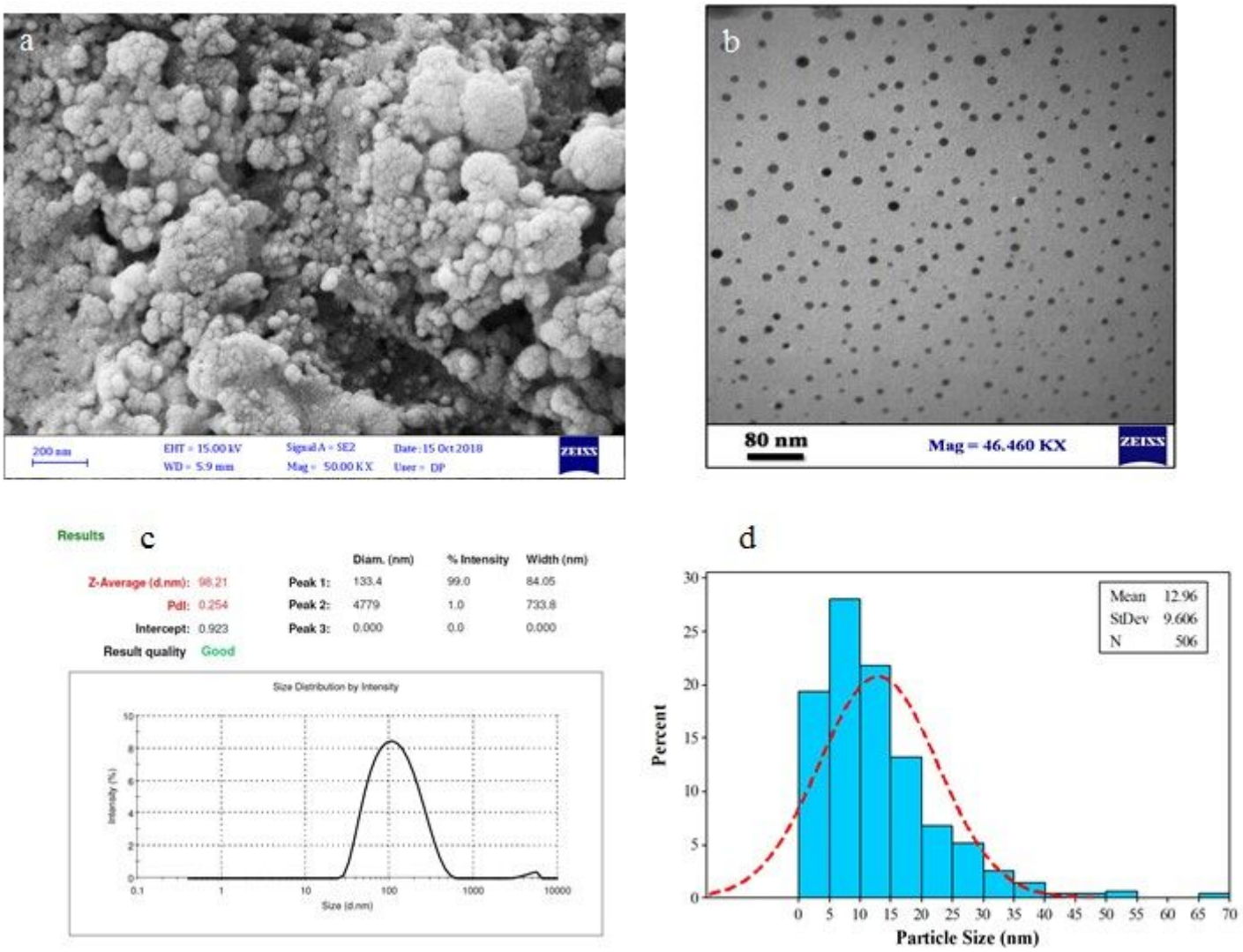

Figure 2

a) SEM analysis of AgNPs synthesized using green method in optimal conditions, b) TEM micrographs of synthesized AgNPs using green synthesis method, c) DLS analysis and d) histogram of particles size.

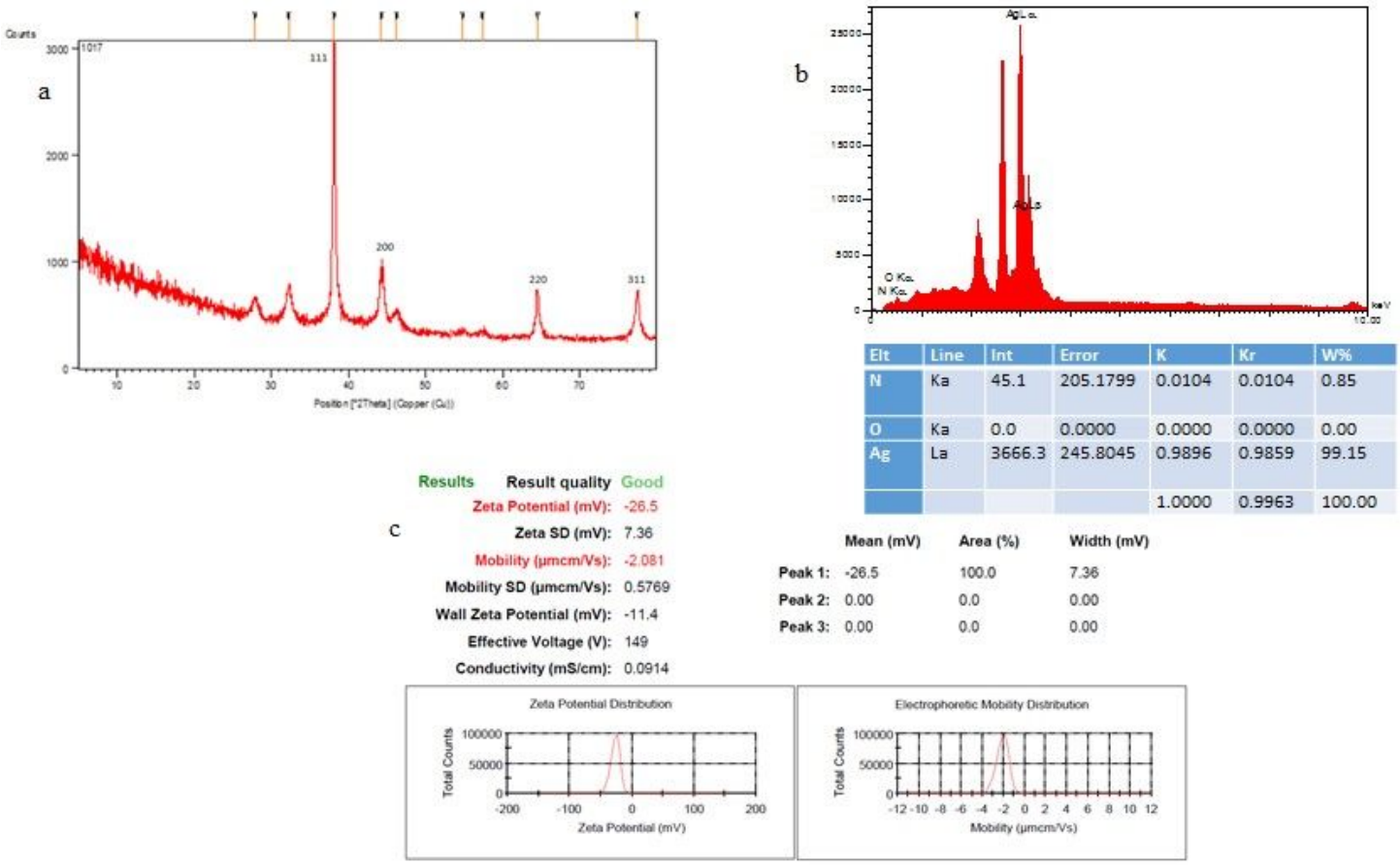

Figure 3

a) XRD pattern of AgNPs synthesized using Juniperus polycarpos extract. b) EDS spectrum of silver nanoparticles synthesized by Juniperus polycarpos. C) Zeta potential of synthesized AgNPs fabricated using aqueous leaf extract of Juniperus polycarpos.

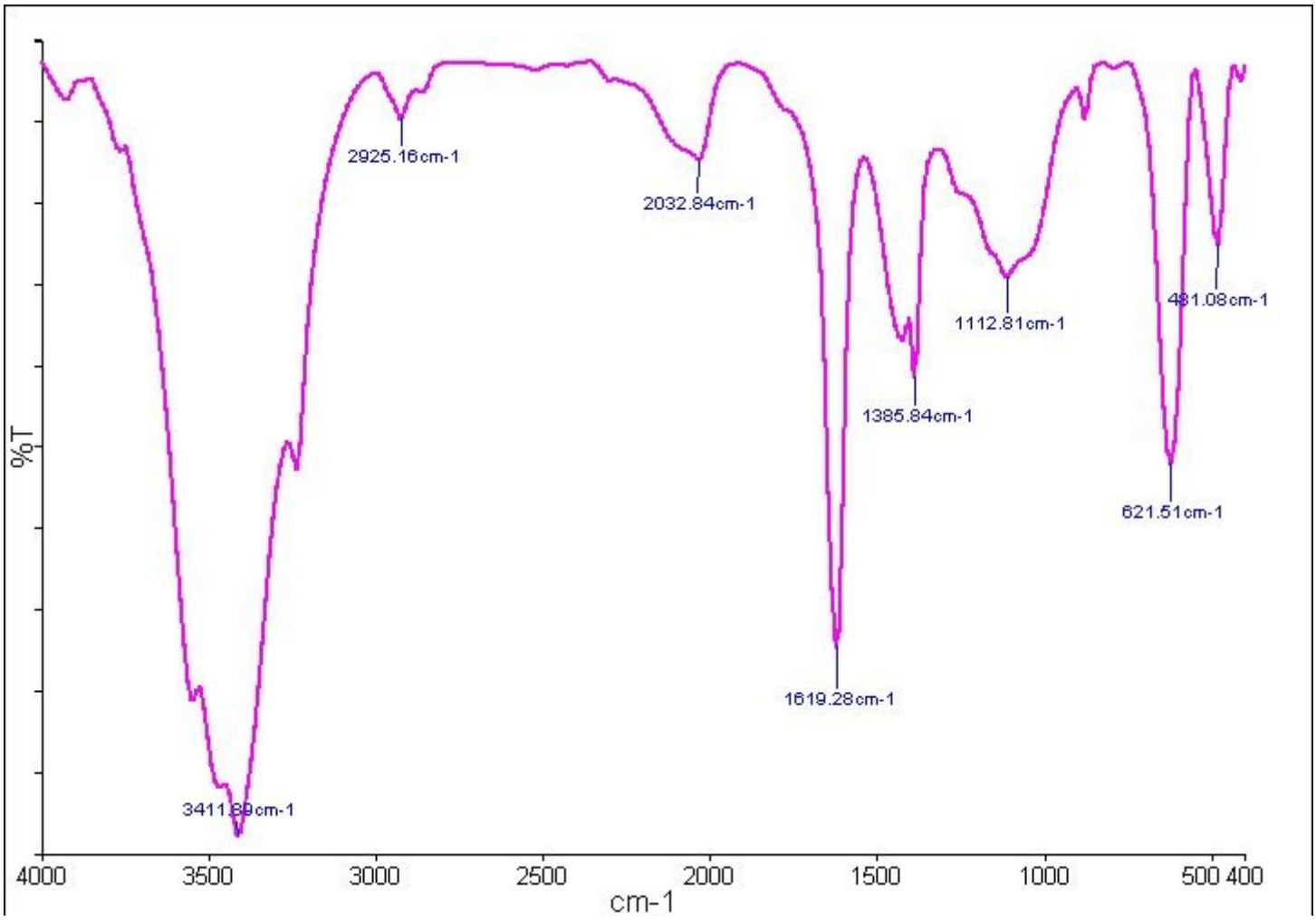

Figure 4

Indicates the FTIR spectrum of the synthesized AgNPs by Juniperus polycarpos extract.

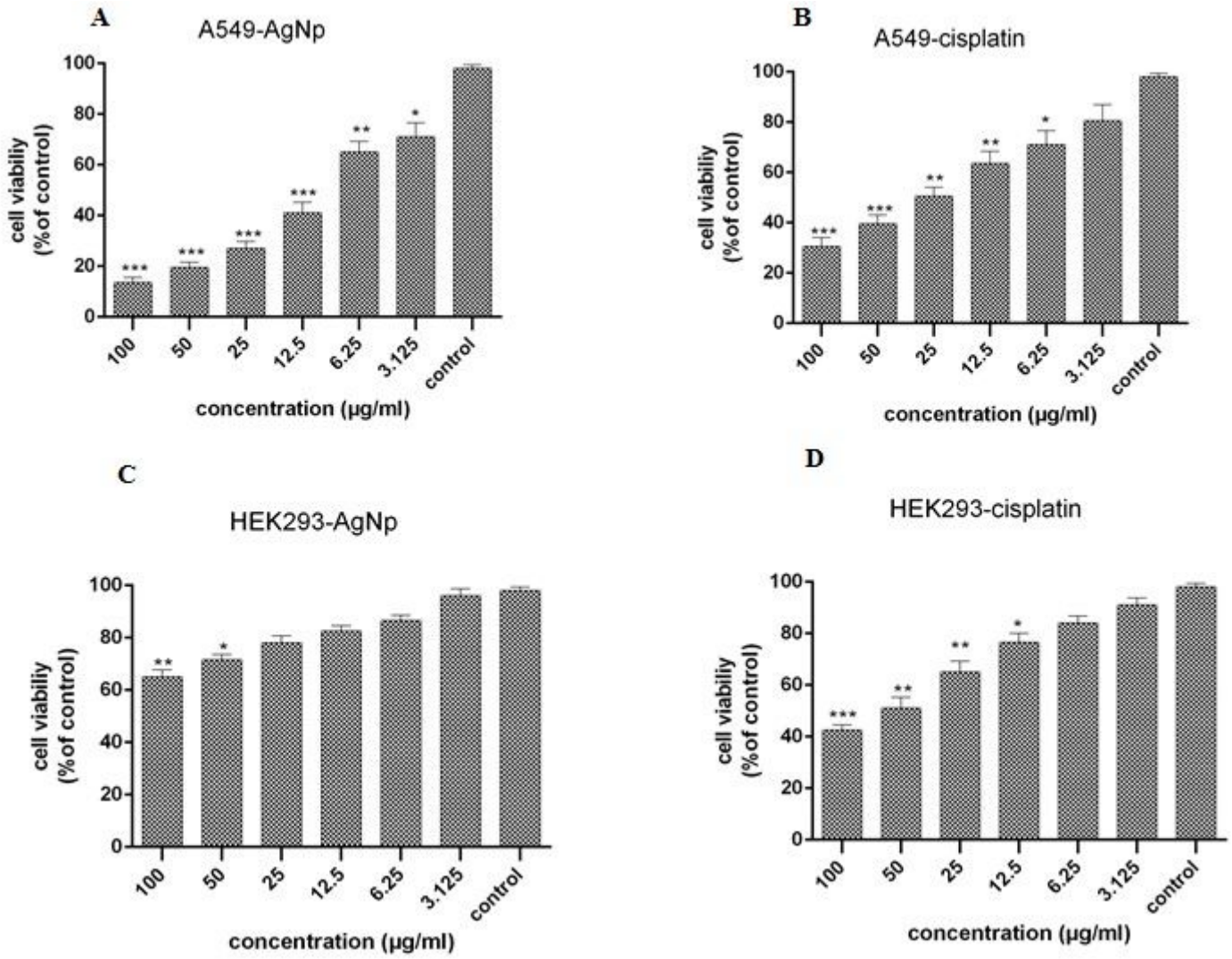

Figure 5

Viability of A549 and HEK293 Cells Exposed different concentration of bio-synthesized AgNPS and cisplatin in Cell Culture. * indicate significant difference compared with control. (***:P<0.001, **:P<0.01 and **:P<0.05).

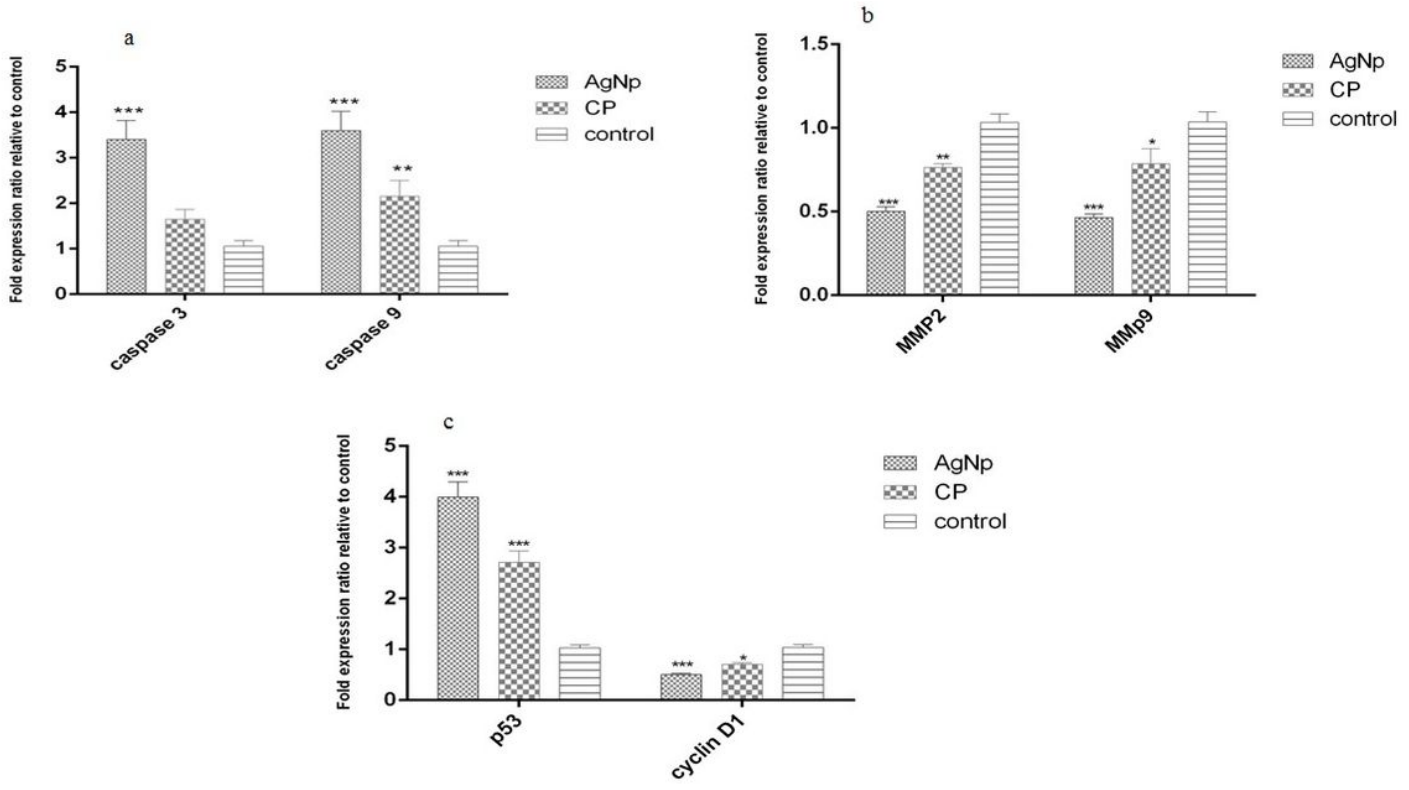

Figure 6

Expression levels of caspase-3, caspase-9, MMP2, MMP9 and p53 and cyclin D1 genes exposed to bio-synthesize AgNPs and cisplatin. (***:P<0.001 and **:P<0.01).

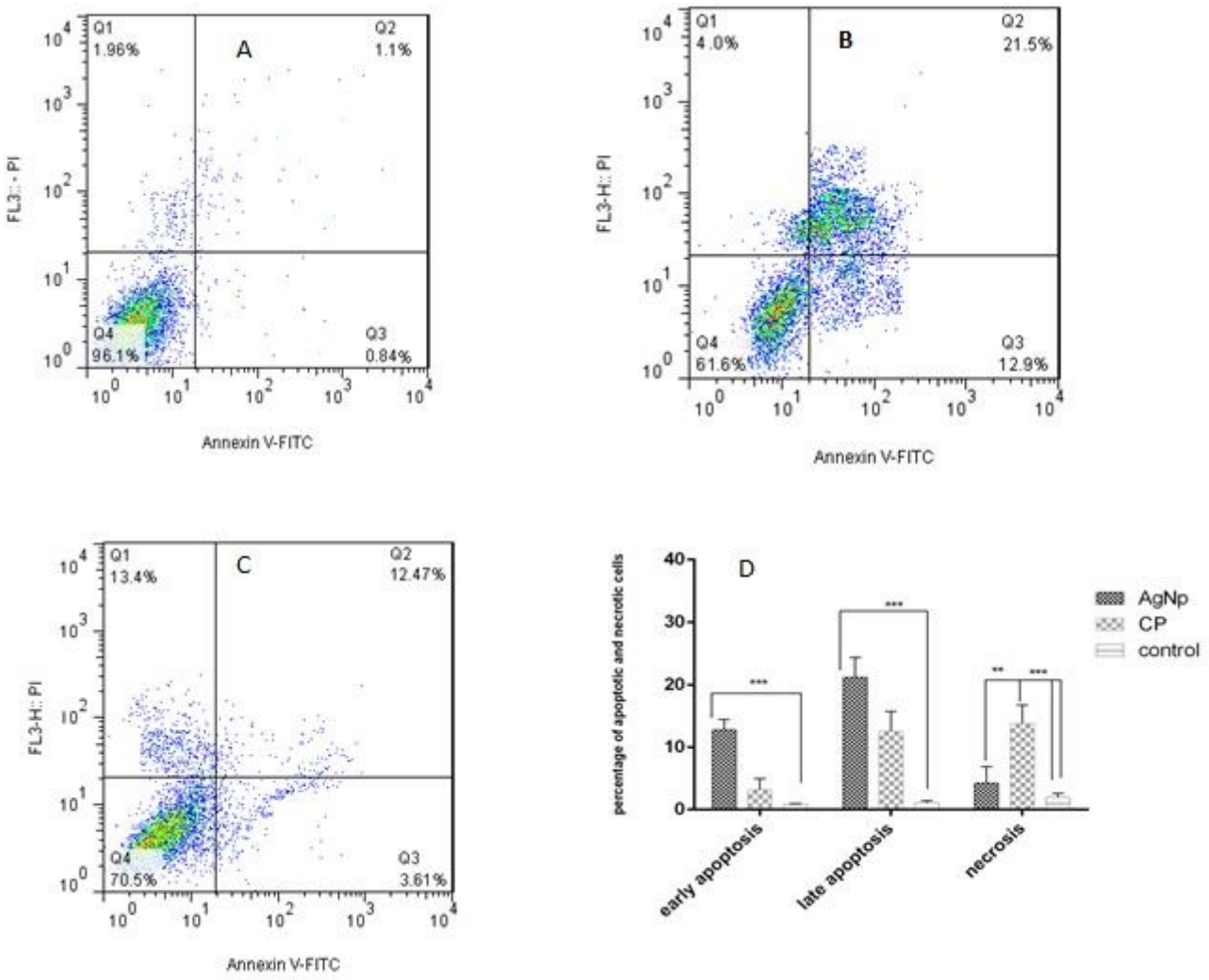

Figure 7

Flow cytometric analysis by Annexin V-FITC in the y-axis and PI (FL3) in the x-axis double staining of A549 cell line treated with green synthesised AgNPs and cisplatin after 24 h exposure. Dot plots of Annexin V/PI staining are shown in (a) Untreated A549 cells, (b) A549 cells treated with IC50 concentration of AgNPs. (c) A549 cells treated with IC50 concentration of cisplatin.

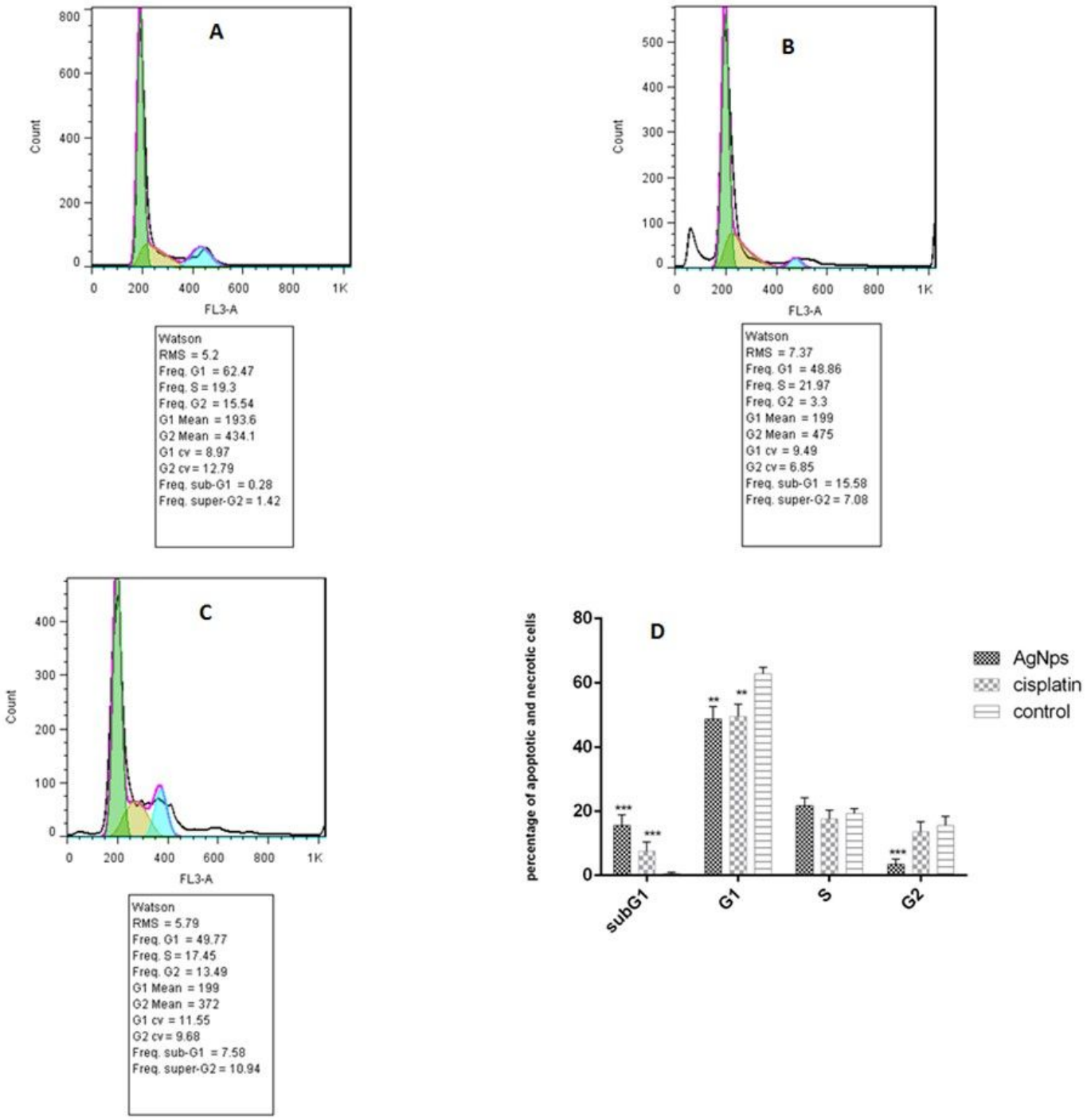

Figure 8

Cell cycle analysis using flow cytometry. (A) control cells, (B) AgNp treated cells, (C) cisplatin treated cells. The initial, middle, and last peaks represent subG1, G1, S and G2, respectively. (D) Bar chart depicting the percentage of resistant cells in subG1, G1, S and G2. (**p < 0.01, and ***p < 0.001).

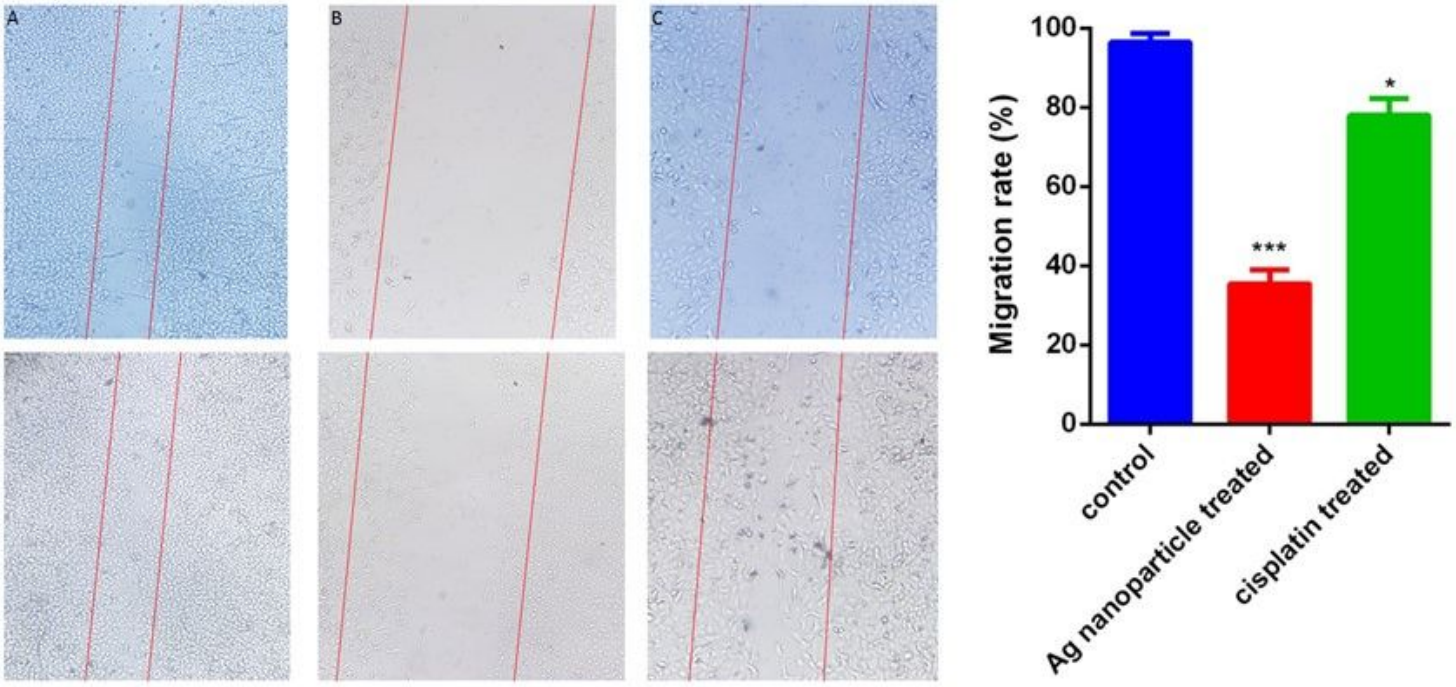

Figure 9

Inhibition of A549 lung cancer cell lines migration in an “in vitro wound-healing” assay. (A) untreated control cells, (B) treated cells with AgNPs and (C) treated cells with cisplatin for 24 h. Bar chart depicting the number of migrated cells per field The results were obtained from triplicate experiments and are presented the mean ± standard deviation (n=3). (*p < 0.05, and ***p < 0.00).

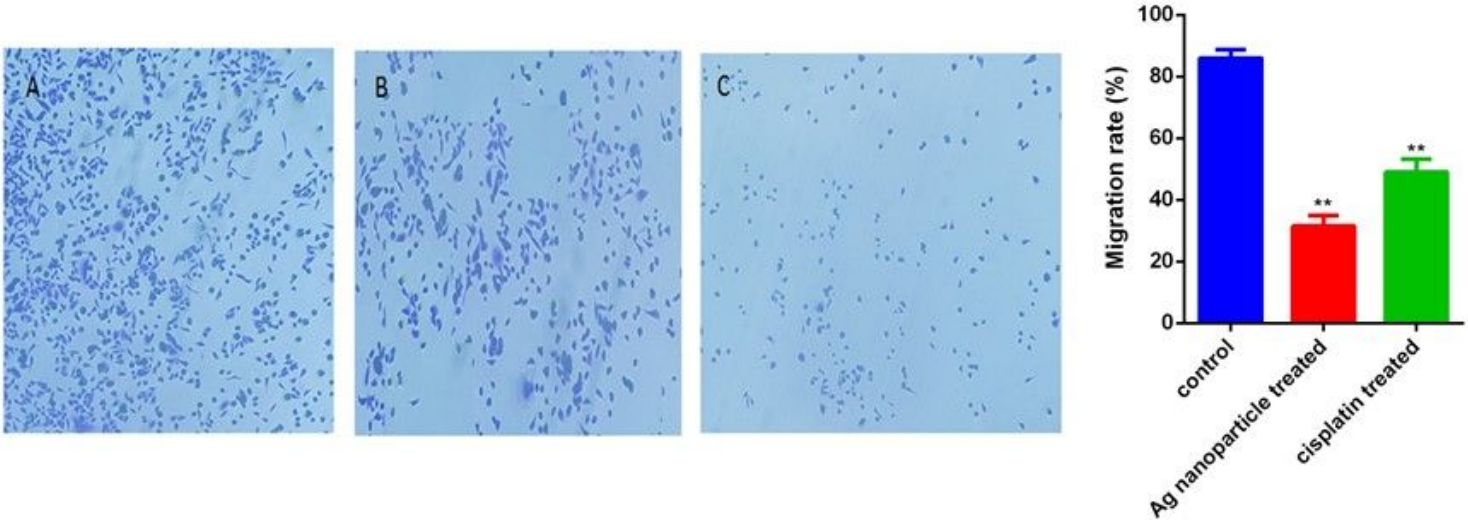

Figure 10

AgNPs and cisplatin reduces cell mobility. (A) Indicates the invasion rate in control cells, (B) and revealed the invasion rate A549 cells were treated with cisplatin (C) shows the invasion rate in A549 cells were treated with AgNPs for 24 h. The results were obtained from triplicate experiments and are presented the mean ± standard deviation (n=3). **p < 0.01.

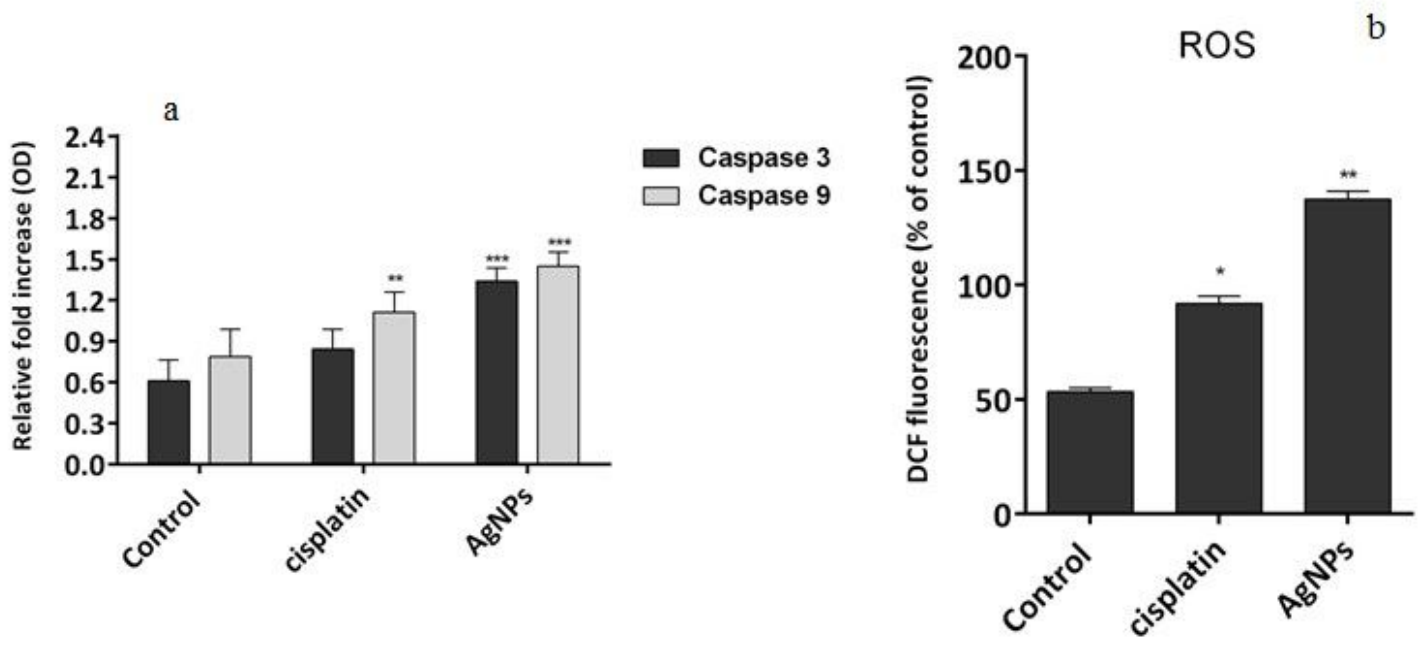

Figure 11

Effect of silver and cisplatin nanoparticles synthesized from Juniperus polycarpos on caspases (A) and ROS production (C) in A549 lung carcinoma cell line. Each bar represents mean ± SEM of three independent observations. *P<0.05 and **P<0.01 are considered as statistically significant.

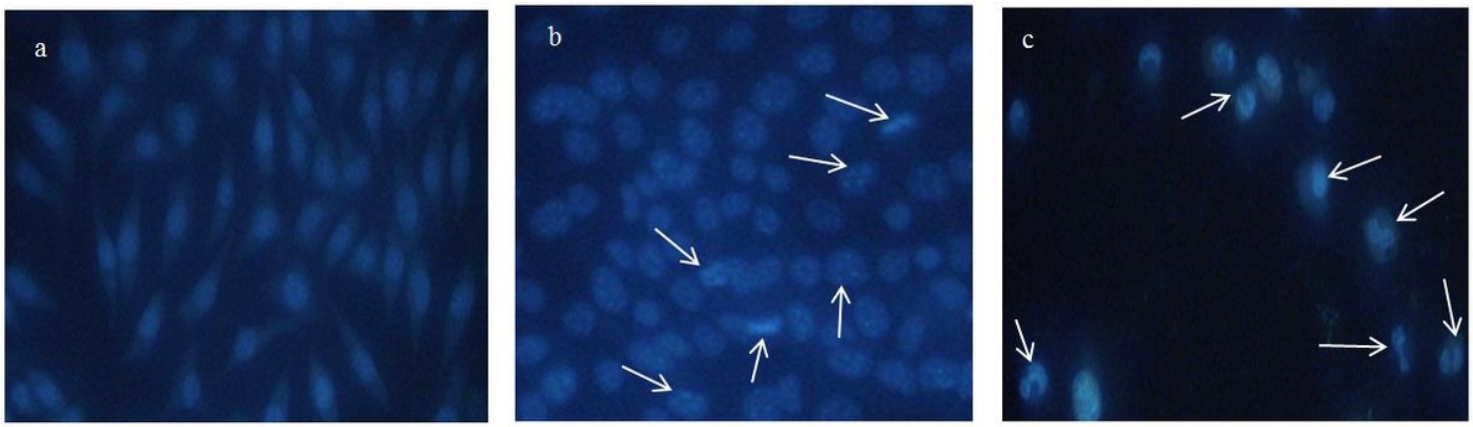

Figure 12

DAPI nuclear staining, a) represents control group, b) represents the group that treated with cisplatin, c) cell treated with cisplatin.